Lens and IOL Tilt

61

Nino Hirnschall and Oliver Findl

Tilt and Visual Quality

A tilt of an intraocular lens (IOL) reduces optical quality due to an increase of lower [1, 2] and higher order aberrations [3]. The impact of tilt on positive and negative dysphotopsia as well as chromatic aberrations appears to be uncertain [4, 5]. Aberrations are a problem for any kind of IOL, but especially for aspheric [6–9], toric [10, 11], extended depth of focus [12, 13], and multifocal IOLs [3].

In the case of an aspherical IOL, tilt leads to a reduction of the aspherical effect up to a worse performance compared to a spherical IOL [6–9]. A "common" amount of tilt (up to 5°) was not shown to have a relevant influence on the performance of the Strehl ratio in a randomized trial (spherical versus aspherical IOL) [14, 15]. Higher amounts of tilt increase coma (which can mimic astigmatism) [16] and reduce the effect of asphericity [10]. Comparing aspherical, aberration neutral and spherical IOLs in the presence of tilt showed that an aberration neutral IOL outperforms an aspherical IOL [17, 18].

For toric IOLs, tilt has a direct and indirect impact on post-operative astigmatism [10, 11] and it explains approximately 11% of the residual astigmatism error or up to 20% if angle kappa is also taken into account [19].

Multifocal IOLs show a reduced optical quality if tilted. Although this accounts for any type of multifocal IOL, especially the performance of rotationally asymmetric multifocal IOLs decreases with tilt [20, 21].

Measurement of Tilt

Severe tilt may be detected at the slit lamp, although it does not allow any quantification of tilt and the measurement is not reliable.

In general, there are two principal methods to quantify tilt:

1. Cross-sectional scans of the anterior segment
   - Scheimpflug imaging or rotating slit lamp images
   - Optical coherence tomography (OCT)
   - Ultrasound biomicroscopy (UBM)
2. Assessing the Purkinje reflexes

N. Hirnschall
Department for Ophthalmology and Optometry, Kepler University Hospital GmbH and Medical Department Johannes Kepler University Linz, Linz, Austria
e-mail: nino@hirnschall.at

O. Findl (✉)
Vienna Institute for Research in Ocular Surgery (VIROS), A Karl Landsteiner Institute, Hanusch Hospital, Vienna, Austria
e-mail: oliver@findl.at

J. Aramberri et al. (eds.), *Intraocular Lens Calculations*, Essentials in Ophthalmology,
https://doi.org/10.1007/978-3-031-50666-6_61

Cross Section-Based Imaging

Tilt quantification with cross-sectional images was introduced in the 1980s [22]. Due to the fact that conventional imaging techniques (except ultrasound) use a light source, imaging behind the iris is not possible. Therefore, this type of tilt quantification uses a fitting concept, where the visible parts of the anterior and posterior lens surfaces are fitted using curved lines (Fig. 61.1). The point of contact is then the estimated equator of the lens. This kind of measurement needs to be performed with a well-dilated pupil in order to assess as much surface of the IOL as possible. In some cases, it is also difficult to identify the anatomical structures of the eye that are necessary to align the points of the reference axis [23].

More recently, OCT devices have been used to quantify tilt. This concept was shown to be successful for older concepts, such as the time domain OCT [24], but also for more modern devices, such as longitudinal B scans using a swept source OCT [25], or anterior segment swept source OCT devices [26]. Fig. 61.1

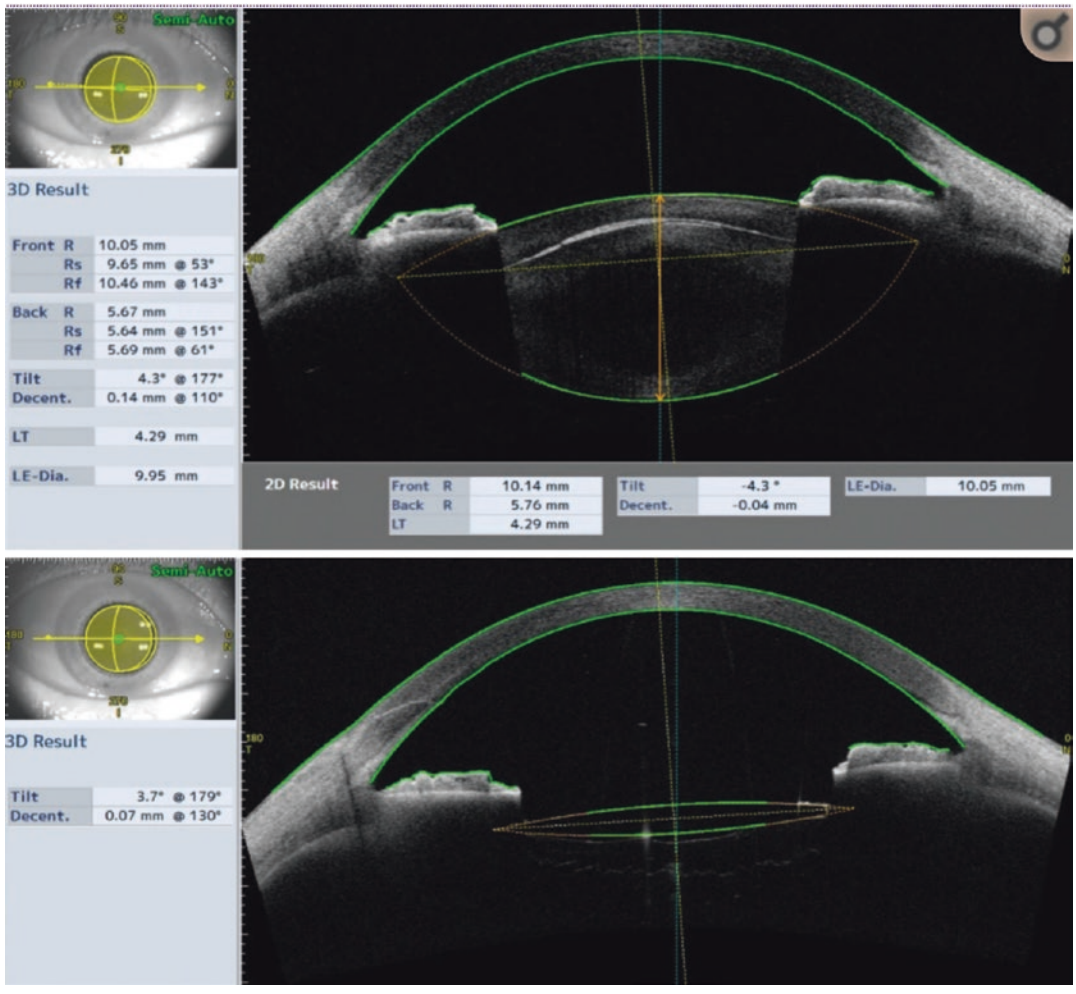

Fig. 61.1 ssOCT images of the phakic (above) and pseudophakic eye (below). The anterior/posterior surfaces of the cornea and the lens are automatically detected [27]

shows the large imaging range of up to 13 mm width that allows to measure the region between the epithelium of the cornea and the posterior lens capsule in a single scan [27]. Additionally, tilt was also quantified using a 3-dimensional approach [28–30] and a deep learning approach was introduced that allowed to automatically quantify tilt using the scleral spur as a reference [31].

Another possibility is to use a high resolution ultrasound device, often referred to as ultrasound biomicroscopy (UBM), which allows measurements behind the iris [32]. A disadvantage of UBM is that a probe is needed and while the eye is in contact with the probe, the patient cannot fixate on a target. However, it is a good approach for cases where low compliance levels are expected [33]. Although it is more difficult to define the reference axis for UBM scans, it was shown to be beneficial for quantification of out of the bag IOL implantation [34–37].

Purkinje Reflexes

Purkinje reflexes are another possibility to assess tilt. This concept was already used in the early 1980s [38–40]. Since light is reflected at all interfaces of media with a difference in refractive index, these reflections, called Purkinje reflexes, may be used to assess tilt of IOLs.

Two different clinically applicable Purkinje meter systems have been used for the measurement of IOL decentration and tilt [3, 41]. These Purkinje meters use a different algorithm for the analysis. A video camera-based photograph of the reflections from the cornea and the IOL is performed in both devices and with the help of a dedicated software, tilt is calculated [3]. The technique is a non-contact technique which is quick and easy to perform. The improvement and advancement of both systems have been shown to be accurate to measure IOL alignment and to evaluate the effect of IOL misalignment on optical performance [42].

Tabernero et al. [41] improved the measureability of tilt by using a semicircular ring of light emitting diodes. These semicircles are captured and analysed according to their size and distance to each other as well as their position within the pupil (Fig. 61.2).

Fig. 61.2 Purkinje imaging of a perfectly aligned ophthalmic system—the outer circle represents the pupillary margin, the inner complete dotted circle the first and second (lower half) and the fourth (upper half) Purkinje reflex. The third Purkinje reflex representing the anterior surface of the lens is reflected as a thick dotted half circle [43]

As shown in Fig. 61.2, only three semicircles are visible, because the first and second Purkinje reflex (anterior and posterior surface of the cornea) overlap. The distances between the reflexes and the position within the pupil are then plotted as an angular fixation function, where the fixation angle correspondences with the overlapping point of the third (anterior surface of the lens) and the fourth (posterior surface of the lens) Purkinje reflexes. Due to the fact that the patient fixates a central target, IOL tilt and decentration can be measured. This idea was previously described by Guyton et al. [44] in a more manual fashion that was also confirmed in a later study [45].

Another Purkinje meter was developed by Schaeffel [43] and differs from Tabernero's Purkinje meter in terms of the light source (single LED instead of a semicircle) and the patient has to fixate on an LED target at different positions instead of one central fixation target (Fig. 61.3).

In a direct comparison between both Purkinje meters including 30 eyes and inviting both inventors to assist with the measurements, a higher feasibility for the Purkinje meter developed by Tabernero and Artal was found [46]. Comparing only the successfully measured cases, both devices should not be used interchangeably.

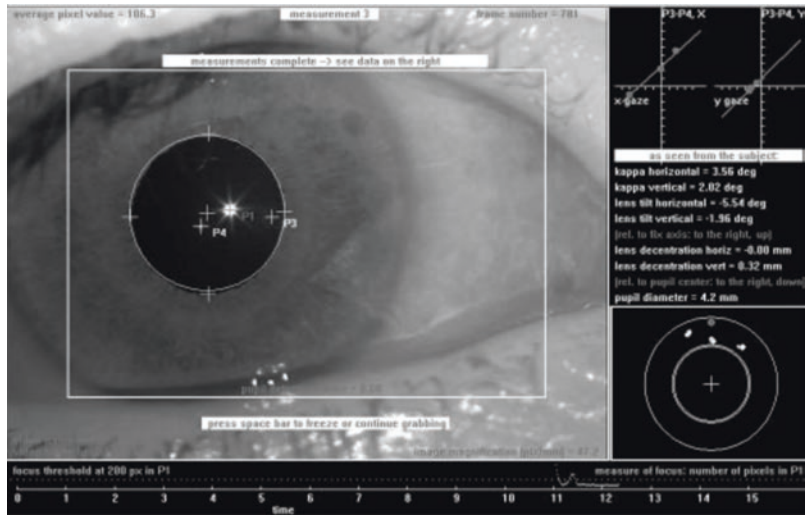

Fig. 61.3 Purkinje meter using dots instead of half circles and an audio system to evaluate the quality of the image [43]

In a direct comparison of Scheimpflug imaging and Purkinje meter measurements, both were shown to be reproducible, but the accuracy was higher for the Purkinje meter measurements [47].

Physiological Tilt

A certain amount of tilt is beneficial, as it compensates for horizontal coma [48]. The mean amount of tilt of the crystalline lens was shown to range between 4.3° [49], 4.6° [43], 4.9° [27], and 5.2° [50]. Furthermore, there is a correlation between axial eye length and tilt with shorter eyes having a higher amount of tilt [25, 51]. This should be kept in mind and the term "physiological tilt" should be introduced. There is evidence that the physiological tilt is inferotemporal (the fovea is slightly temporal to the pupillary axis) [49–51] and that there is a mirror-symmetry between the eyes [49]. Furthermore, tilt slightly increases (on average less than 0.5°) in the presence of mydriasis [50].

For IOLs, there is a variety of studies assessing the amount of tilt ranging from 2.7° [52], 2.9° [53], 2.9° [28], 3.9° [54], 4.1° [55], 4.8° [51] to 6.2° [49]. Although this list is not complete, it shows the range of tilt. The amount of tilt depends on several factors, such as axial eye length, different measurement and analysis systems, and differences in reference axes. Unfortunately, there is no standardization and different authors have used different definitions and different reference axes so that they cannot be used interchangeably (Fig. 61.4) [56]. This is relevant as some reference axes include angle kappa, whereas others do not [56].

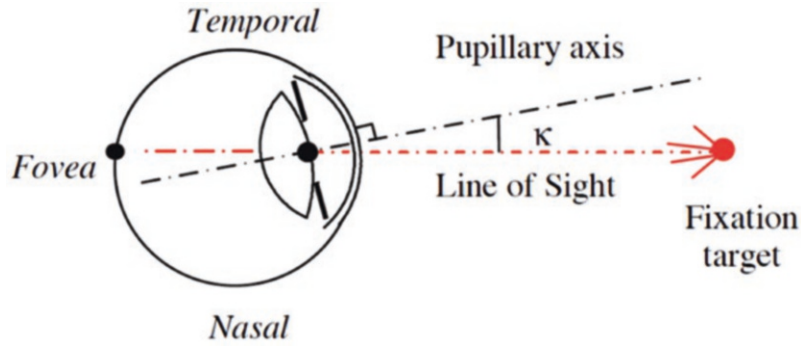

Fig. 61.4 Graphical definition of pupillary axis and line of sight and the angle kappa [41]

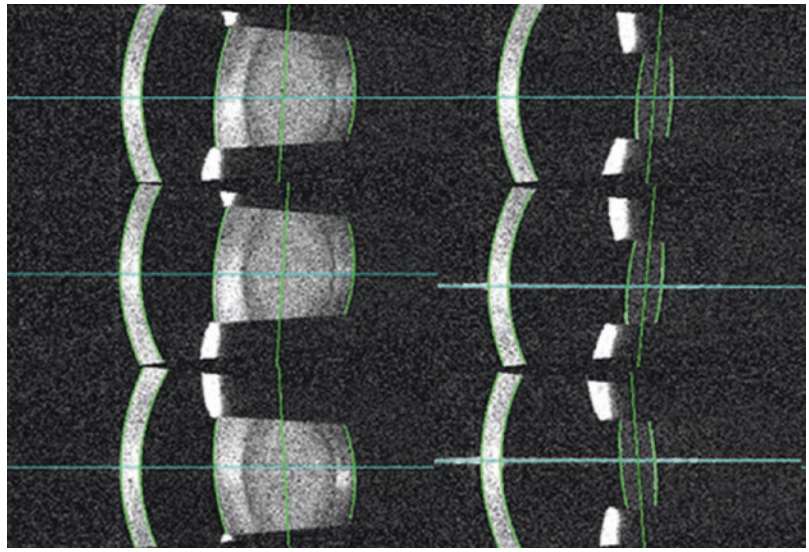

Fig. 61.5 Swept source OCT imaging at three different meridians of the same eye in the phakic state (left) and the pseudophakic state (right) [49]

Prediction of Post-operative Tilt

As mentioned above, tilt accounts for more than 10° of the error in toric IOL power calculation and this value increases to almost 20%, if combined with angle kappa [57]. Therefore, predicting tilt and taking it into account would significantly improve toric IOL power calculation [49, 57, 58].

Although prediction of the post-operative amount of tilt is more difficult (correlation of $r = 0.4$) [49], it was shown that the orientation of tilt can be predicted quite well with a correlation of $r = 0.7$ (Fig. 61.5) [49]. The average orientation before and after cataract surgery is approximately 16–17° and the predictive power is high [49]. The correlation for the pre- to post-operative amount of tilt was found to be higher ($r = 0.5$–0.7) in two other studies (Table 61.1) [25, 27]. Axial eye length was not found to be a good predictor of post-operative tilt ($r = 0.2$) [25].

Table 61.1 Data of pre-operative and post-operative amount of tilt in three different studies. * data not in the paper, but calculated from the associated online .xls file

	Mean Crystalline tilt in ° (SD)	Mean IOL tilt in ° (SD)
Gu et al. [27]	4.9 (1.8)	4.75 (1.66)
Kimura et al. [50]	5.15 (1.4 *)	4.31 (1.7 *)
Wang [25]	3.7 (1.1)	4.9 (1.8)
Hirnschall et al. [49]	4.3 (0.9)	6.2 (1.3)

Factors Influencing Tilt

Although there is currently no good prediction algorithm on which eye will have severe IOL tilt after cataract surgery, several risk factors were discussed.

Capsulorrhexis

Different aspects of the capsulorrhexis were evaluated concerning their impact on IOL tilt. There is good evidence that the size of the capsulorrhexis has no influence on IOL tilt [55, 59]. Shape and centration of the rhexis were also not found to be clinically relevant in the same two studies. However, an incomplete capsulorrhexis overlap (probably less than 50% overlap—estimation) was found to be a risk factor for tilt [55, 59, 60]. Older techniques used before the introduction of the continuous curvilinear capsulorrhexis, such as the envelop technique, resulted in significantly higher tilt values and should be avoided [61].

As the size and shape of the capsulorrhexis were not shown to have a relevant impact on tilt with modern single-piece IOLs (except for a severe missing overlap), it is likely that femtosecond laser-assisted cataract surgery (FLACS) does not reduce post-operative tilt either. However, it should be mentioned that this was not confirmed in all studies [62].

The bag-in-the-lens IOLs, where the IOL is connected to the anterior and posterior capsulorrhexis edges, were shown to have small amounts of tilt [63, 64]. Although this type of IOL may be used with a meticulously made manual capsulorrhexis, it may be easier to be used with a FLACS made capsulotomy, as the shape and the size of the capsular opening are crucial for the position of the IOL. Incision size was not found to be a relevant factor for predicting tilt [65, 66].

Pseudoexfoliation

Pseudoexfoliation was found to be a relevant risk factor for a post-operative forward tilting of the superior haptic [24, 67, 68] as well as a long-term risk factor for IOL dislocation [69, 70]. Furthermore, pseudoexfoliation is associated with anterior capsule contraction syndrome, which may also result in a tilted IOL [71].

In another study, there was a tendency that a capsular tension ring prevents tilt to a certain degree [72]. This could be beneficial in eyes with pseudoexfoliation, but evidence is scarce and further studies would be necessary for confirmation.

IOL Material and Design

There is general agreement that the influence of IOL material has no or only a minor impact on IOL tilt [73–75]. Walkow et al. [76] observed similar results, when assessing the reason for IOL explantation due to decentration or subluxation.

On the other side, the design of the haptics was found to be relevant [73]. This leads to the question, if there is a difference between 1-piece and 3-piece IOLs. A large randomized bilateral comparison found significant differences with the 3-piece IOL showing a significantly higher amount of tilt [53]. This was also confirmed by another randomized trial [53]. Two other studies did not confirm this finding [52, 77]. Although the design of the haptics potentially has an effect on the amount of tilt, the orientation of the haptic position was not found to be relevant [53].

Possibly, the higher tilt in 3-piece designs is a consequence of a slight kinking or bending of the haptic during the implantation process since the haptics have a limited memory compared to the thicker single-piece haptics used.

After-Cataract

Although only mild in extent, posterior capsule opacification, or after-cataract, potentially increases tilt and may be relieved with a posterior Nd:YAG capsulotomy which was shown to decrease tilt back to normal levels [78, 79].

IOL Implantation Outside the Capsular Bag

Three piece IOLs in the sulcus tend to have higher tilt levels (horizontal tilt on average 7.7°) compared to those in the bag IOLs [80]. If this is due to the position in the sulcus itself, or due to the typically compromised posterior capsule has not been identified. Another explanation could be that in the case of sulcus IOLs sometimes one of the haptics unintentionally is positioned in the bag instead of being in the sulcus [37].

For scleral fixated IOLs, slightly higher tilt values were observed compared to those in the bag IOL implantation. For scleral fixated IOLs with a Z-suture, relevant tilt was found in 72% of all cases [81], whereas intrascleral fixation showed lower tilt values of little more than 3°, even though 8% of all cases had an iris capture [82]. Low tilt values were also confirmed for self-sealing scleral pockets measured with UBM [34–36] and OCT technology [35] and for long-term results using glue [83].

Furthermore, scleral fixated IOLs showed less tilt, if the sclerectomy was performed with 24 gauge compared to 30 gauge [84]. In the case of relevant post-operative tilt shortening, the length of the haptics was found to be useful to reduce tilt in some cases [85]. There is little information comparing tilt data of scleral fixated IOLs versus iris claw IOLs. One study performed in children showed higher tilt values for scleral fixated IOLs [86].

Combined Surgery

For phacotrabeculectomy, there is no evidence for an increased risk of clinically relevant IOL tilt [87]. Phacovitrectomy potentially increases the risk of IOL tilt, depending on the vitreous tamponade [51]. If air or gas is used, there is evidence for an increased tilt compared to no tamponade [26, 88, 89]. However, this difference was not found to have a significant influence on lower or higher order aberrations and the clinical effect is questionable [88]. It should also be mentioned that a randomized study directly comparing combined phacovitrectomy including endotamponade versus cataract surgery as a stand-alone procedure did not confirm these findings and no difference in tilt was observed [90].

Effect of Tilt on Refraction

The effect of tilt on the induced astigmatism in an aspherical toric IOL depends on several variables:

- Power of the IOL (spherical equivalent and astigmatism if the lens is toric)
- Amount and orientation of tilt

As shown by Weikert et al. [10], a non-toric aspheric IOL tilted horizontally (nasal border more anterior, like physiological tilt) will induce against the rule astigmatism. A horizontal tilt of 10° of a 16D and a 28D IOL would result in an induced against the rule astigmatism of 0.33D and 0.56D, respectively (Fig. 61.6).

In the case of a toric IOL oriented at 90°, the horizontal tilt resulted in increased against the rule astigmatism, resulting in overcorrection. If the IOL was oriented at 180°, the consequence would be an undercorrection. It's curious to observe that this against the rule trend is similar to the effect of the posterior corneal surface astigmatism.

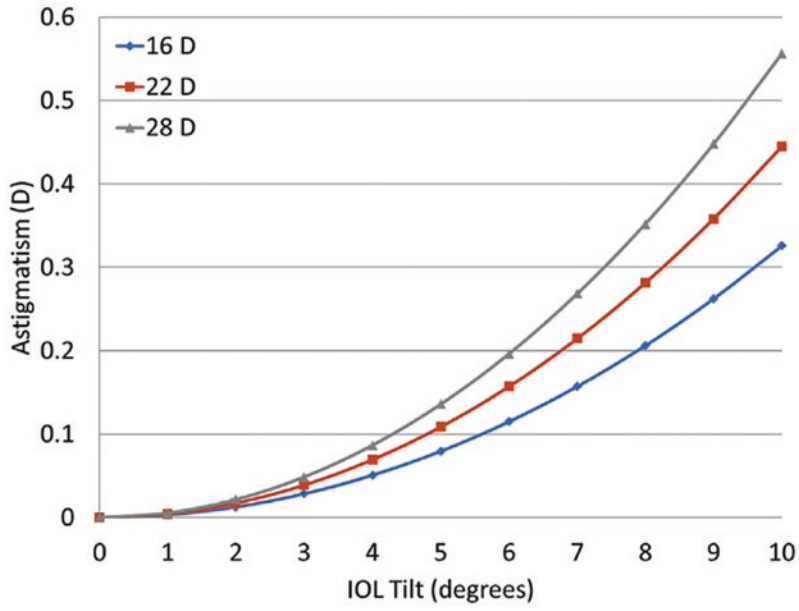

Fig. 61.6 Simulated against the rule astigmatism induced by tilt in an eye with an aspheric IOL for three different IOL powers [10]

Marcos presented a method to estimate the effect of tilt on astigmatism (in air) using a thin lens formula (Eq. 61.1).

$$A = P\left\{1+\frac{(\sin\alpha)^2}{3}\right\} * (\tan\alpha)^2 \qquad (61.1)$$

Estimating the effect of tilt on astigmatism (A = astigmatism in D, P = power of the IOL in D, α = amount of tilt [91].

A more complex approach would be to use a model with a thin spherical lens. Simplifying the model by neglecting all effects above the second order of aberrations, the Coddington formula may be used [92]. The effect of tilt has to be explained for each order of aberration. Atchison published a thin lens calculation for the effect of tilt on first- and second-order aberrations [92]. According to the Coddington formula, a finite principal ray is sent from an object through a spherical lens and another neighboured ray is sent from the same object through the same lens, where these two rays intersect after refraction [93]. This intersection point consists of focal lines. The two main focal lines are usually called tangential (V_T) and sagittal (V_S) (Eq. 61.2).

$$V_S : \frac{n'}{s'} = \frac{n}{s} + (n'\cos I' - n\cos I)c_S$$
$$V_T : \frac{n'\cos^2 I'}{t'} = \frac{n\cos^2 I}{t} + \frac{n'\cos I' - n\cos I}{r} \qquad (61.2)$$

Vergence for tangential (V_T) and sagittal (V_S) focal lines [93].

s and t = distance from the incident point of the ray to the sagittal and tangential point of the image.

c_S = curvature of the anterior lens surface.

I and I' = angles of incidence and refraction.

n and n' = refractive indices of the object and image spaces (n represents the refractive index of the object side medium and n' represents the refractive index of the image side medium).

In a very similar fashion, V_T' can be calculated using the Coddington formula for V_T, as shown in Eq. (61.3).

$$V_T' = V + \left(1+\delta^2+\frac{n\delta^2}{2\delta}\right)F \qquad (61.3)$$

Vergence for the transversally misaligned focal line [92] (modified).

As for the longitudinal displacement, the formula for the effective lens power can be used (Eq. 61.4).

$$V_{CS} = \frac{V_S'}{1 + \frac{dV_S'}{n}} \text{ and } V_{CT} = \frac{V_T'}{1 + \frac{dV_T'}{n}} \quad (61.4)$$

Converted using the effective lens power [92] (modified) V_{CS}=Vergence of the sagittally misaligned lens on the corneal plane.

V_{CT} = Vergence of the transversally misaligned lens on the corneal plane.

The refractive error is, similar to the longitudinal displacement, the difference between the correct position of the lens and the displaced image of the lens ($V_C - V_{CS}$; $V_C - V_{CT}$).

In a next step, these estimations of the refractive error can be combined to explain the spherical equivalent of the refractive error due to lens displacement (Eq. 61.5).

$$\Delta F_{SE} = \Delta F + \Delta F_S + \frac{\Delta F_T}{2} \quad (61.5)$$

Effect of longitudinal misalignment and tilt on the spherical equivalent.

This concept [92] was evaluated using tilt, pseudophakic ACD and refraction data of 100 eyes. The correlation between the theoretically predicted refractive error and the actually measured refractive error using subjective and objective refraction was found to be only moderate (r^2 = 0.42 (not published)). The most likely reason is the low accuracy of the post-operative manifest refraction.

Summary

Physiological tilt shows a mirror symmetry between both eyes, depends on the axial eye length, is orientated inferotemporally, and does not exceed 5°.Tilt above this physiological level has a significant impact on visual quality, especially for aspheric, toric, and multifocal IOLs. Predicting post-operative tilt was shown to be successful and to improve toric IOL power calculation. There are two concepts for tilt measurements, cross-sectional-based scans (Scheimpflug, OCT, UBM) and imaging of the Purkinje reflexes of the eye. Risk factors for tilt are pseudoexfoliation syndrome, 3-piece IOLs, after cataract, and potentially phacovitrectomy with endotamponade. The capsulorrhexis was found to have a minor influence on tilt.

References

1. Hoffer KJ. Astigmatism from lens tilt. J Am Intraocul Implant Soc. 1985;11(1):67.
2. Schroder S, Schrecker J, Daas L, Eppig T, Langenbucher A. Impact of intraocular lens displacement on the fixation axis. J Opt Soc Am A Opt Image Sci Vis. 2018;35(4):561–6.
3. Tabernero J, Piers P, Benito A, Redondo M, Artal P. Predicting the optical performance of eyes implanted with IOLs to correct spherical aberration. Invest Ophthalmol Vis Sci. 2006;47(10):4651–8.
4. Ashena Z, Maqsood S, Ahmed SN, Nanavaty MA. Effect of intraocular lens tilt and decentration on visual acuity, Dysphotopsia and Wavefront aberrations. Vision (Basel). 2020;4(3).
5. Marcos S, Burns SA, Prieto PM, Navarro R, Baraibar B. Investigating sources of variability of monochromatic and transverse chromatic aberrations across eyes. Vis Res. 2001;41(28):3861–71.
6. Lawu T, Mukai K, Matsushima H, Senoo T. Effects of decentration and tilt on the optical performance of 6 aspheric intraocular lens designs in a model eye. J Cataract Refract Surg. 2019;45(5):662–8.
7. Madrid-Costa D, Ruiz-Alcocer J, Perez-Vives C, Ferrer-Blasco T, Lopez-Gil N, Montes-Mico R. Visual simulation through different intraocular lenses using adaptive optics: effect of tilt and decentration. J Cataract Refract Surg. 2012;38(6):947–58.
8. McKelvie J, McArdle B, McGhee C. The influence of tilt, decentration, and pupil size on the higher-order aberration profile of aspheric intraocular lenses. Ophthalmology. 2011;118(9):1724–31.
9. Fisus AD, Hirnschall ND, Maedel S, Fichtenbaum M, Draschl P, Findl O. Capsular bag performance of a novel hydrophobic acrylic single-piece intraocular lens: two-year results of a randomised controlled trial. Eur J Ophthalmol. 2020;31:1120672120960591.
10. Weikert MP, Golla A, Wang L. Astigmatism induced by intraocular lens tilt evaluated via ray tracing. J Cataract Refract Surg. 2018;44(6):745–9.
11. Felipe A, Artigas JM, Diez-Ajenjo A, Garcia-Domene C, Peris C. Modulation transfer function of a toric intraocular lens: evaluation of the changes produced by rotation and tilt. J Refract Surg. 2012;28(5):335–40.
12. Georgiev S, Palkovits S, Hirnschall N, Doller B, Draschl P, Findl O. Visual performance after bilat-

eral toric extended depth-of-focus intraocular lens exchange targeted for micro-monovison. J Cataract Refract Surg. 2020;46:1346.
13. Georgiev S, Palkovits S, Hirnschall N, Doller B, Draschl P, Findl O. Visual performance after bilateral toric extended depth-of-focus IOL exchange targeted for micromonovision. J Cataract Refract Surg. 2020;46(10):1346–52.
14. Baumeister M, Buhren J, Kohnen T. Tilt and decentration of spherical and aspheric intraocular lenses: effect on higher-order aberrations. J Cataract Refract Surg. 2009;35(6):1006–12.
15. Rosales P, De Castro A, Jimenez-Alfaro I, Marcos S. Intraocular lens alignment from purkinje and Scheimpflug imaging. Clin Exp Optom. 2010;93(6):400–8.
16. Perez-Gracia J, Varea A, Ares J, Valles JA, Remon L. Evaluation of the optical performance for aspheric intraocular lenses in relation with tilt and decenter errors. PLoS One. 2020;15(5):e0232546.
17. Eppig T, Scholz K, Loffler A, Messner A, Langenbucher A. Effect of decentration and tilt on the image quality of aspheric intraocular lens designs in a model eye. J Cataract Refract Surg. 2009;35(6):1091–100.
18. Pieh S, Fiala W, Malz A, Stork W. In vitro strehl ratios with spherical, aberration-free, average, and customized spherical aberration-correcting intraocular lenses. Invest Ophthalmol Vis Sci. 2009;50(3):1264–70.
19. Hirnschall N, Findl O, Bayer N, Leisser C, Norrby S, Zimper E, Hoffmann P. Sources of error in toric intraocular lens power calculation. J Refract Surg. 2020;36:646.
20. Liu X, Xie L, Huang Y. Effects of decentration and tilt at different orientations on the optical performance of a rotationally asymmetric multifocal intraocular lens. J Cataract Refract Surg. 2019;45(4):507–14.
21. Montes-Mico R, Lopez-Gil N, Perez-Vives C, Bonaque S, Ferrer-Blasco T. In vitro optical performance of nonrotational symmetric and refractive-diffractive aspheric multifocal intraocular lenses: impact of tilt and decentration. J Cataract Refract Surg. 2012;38(9):1657–63.
22. Sasaki K, Sakamoto Y, Shibata T, Nakaizumi H, Emori Y. Measurement of postoperative intraocular lens tilting and decentration using Scheimpflug images. J Cataract Refract Surg. 1989;15(4):454–7.
23. Baumeister M, Neidhardt B, Strobel J, Kohnen T. Tilt and decentration of three-piece foldable high-refractive silicone and hydrophobic acrylic intraocular lenses with 6-mm optics in an intraindividual comparison. Am J Ophthalmol. 2005;140(6):1051–8.
24. Burgmuller M, Mihaltz K, Schutze C, Angermann B, Vecsei-Marlovits V. Assessment of long-term intraocular lens (IOL) decentration and tilt in eyes with pseudoexfoliation syndrome (PES) following cataract surgery. Graefes Arch Clin Exp Ophthalmol. 2018;256(12):2361–7.
25. Wang L, Guimaraes de Souza R, Weikert MP, Koch DD. Evaluation of crystalline lens and intraocular lens tilt using a swept-source optical coherence tomography biometer. J Cataract Refract Surg. 2019;45(1):35–40.
26. Sato T, Korehisa H, Shibata S, Hayashi K. Prospective comparison of intraocular lens dynamics and refractive error between phacovitrectomy and phacoemulsification alone. Ophthalmol Retina. 2020;4(7):700–7.
27. Gu X, Chen X, Yang G, et al. Determinants of intraocular lens tilt and decentration after cataract surgery. Ann Transl Med. 2020;8(15):921.
28. Wang X, Dong J, Wang X, Wu Q. IOL tilt and decentration estimation from 3 dimensional reconstruction of OCT image. PLoS One. 2013;8(3):e59109.
29. Ding X, Wang Q, Chang P, et al. The repeatability assessment of three-dimensional capsule-intraocular lens complex measurements by means of high-speed swept-source optical coherence tomography. PLoS One. 2015;10(11):e0142556.
30. Li L, Wang K, Yan Y, Song X, Liu Z. Research on calculation of the IOL tilt and decentration based on surface fitting. Comput Math Methods Med. 2013;2013:572530.
31. Xin C, Bian GB, Zhang H, Liu W, Dong Z. Optical coherence tomography-based deep learning algorithm for quantification of the location of the intraocular lens. Ann Transl Med. 2020;8(14):872.
32. Ang GS, Duncan L, Atta HR. Ultrasound biomicroscopic study of the stability of intraocular lens implants after phacoemulsification cataract surgery. Acta Ophthalmol. 2012;90(2):168–72.
33. Zhao YE, Gong XH, Zhu XN, et al. Long-term outcomes of ciliary sulcus versus capsular bag fixation of intraocular lenses in children: an ultrasound biomicroscopy study. PLoS One. 2017;12(3):e0172979.
34. Marianelli BF, Mendes TS, de Almeida Manzano RP, Garcia PN, Teixeira IC. Observational study of intraocular lens tilt in sutureless intrascleral fixation versus standard transscleral suture fixation determined by ultrasound biomicroscopy. Int J Retina Vitreous. 2019;5:33.
35. Boral SK, Agarwal D. A simple modified way of Glueless, Sutureless scleral fixation of an IOL: a retrospective case series. Am J Ophthalmol. 2020;218:314–9.
36. Mura JJ, Pavlin CJ, Condon GP, et al. Ultrasound biomicroscopic analysis of iris-sutured foldable posterior chamber intraocular lenses. Am J Ophthalmol. 2010;149(2):245–52 e2.
37. Vasavada AR, Raj SM, Karve S, Vasavada V, Vasavada V, Theoulakis P. Retrospective ultrasound biomicroscopic analysis of single-piece sulcus-fixated acrylic intraocular lenses. J Cataract Refract Surg. 2010;36(5):771–7.
38. Phillips P, Perez-Emmanuelli J, Rosskothen HD, Koester CJ. Measurement of intraocular lens decentration and tilt in vivo. J Cataract Refract Surg. 1988;14(2):129–35.
39. Auran JD, Koester CJ, Donn A. In vivo measurement of posterior chamber intraocular lens decentration and tilt. Arch Ophthalmol. 1990;108(1):75–9.

40. Kirschkamp T, Dunne M, Barry JC. Phakometric measurement of ocular surface radii of curvature, axial separations and alignment in relaxed and accommodated human eyes. Ophthalmic Physiol Opt. 2004;24(2):65–73.
41. Tabernero J, Benito A, Nourrit V, Artal P. Instrument for measuring the misalignments of ocular surfaces. Opt Express. 2006;14(22):10945–56.
42. Nishi Y, Hirnschall N, Crnej A, et al. Reproducibility of intraocular lens decentration and tilt measurement using a clinical Purkinje meter. J Cataract Refract Surg. 2010;36(9):1529–35.
43. Schaeffel F. Binocular lens tilt and decentration measurements in healthy subjects with phakic eyes. Invest Ophthalmol Vis Sci. 2008;49(5):2216–22.
44. Guyton DL, Uozato H, Wisnicki HJ. Rapid determination of intraocular lens tilt and decentration through the undilated pupil. Ophthalmology. 1990;97(10):1259–64.
45. Wu M, Li H, Cheng W. Determination of intraocular lens tilt and decentration using simple and rapid method. Yan Ke Xue Bao. 1998;14(1):13–6, 26.
46. Maedel S, Hirnschall N, Bayer N, et al. Comparison of intraocular lens decentration and tilt measurements using 2 Purkinje meter systems. J Cataract Refract Surg. 2017;43(5):648–55.
47. de Castro A, Rosales P, Marcos S. Tilt and decentration of intraocular lenses in vivo from Purkinje and Scheimpflug imaging. Validation study. J Cataract Refract Surg. 2007;33(3):418–29.
48. Marcos S, Rosales P, Llorente L, Barbero S, Jimenez-Alfaro I. Balance of corneal horizontal coma by internal optics in eyes with intraocular artificial lenses: evidence of a passive mechanism. Vis Res. 2008;48(1):70–9.
49. Hirnschall N, Buehren T, Bajramovic F, Trost M, Teuber T, Findl O. Prediction of postoperative intraocular lens tilt using swept-source optical coherence tomography. J Cataract Refract Surg. 2017;43(6):732–6.
50. Kimura S, Morizane Y, Shiode Y, et al. Assessment of tilt and decentration of crystalline lens and intraocular lens relative to the corneal topographic axis using anterior segment optical coherence tomography. PLoS One. 2017;12(9):e0184066.
51. Chen X, Gu X, Wang W, et al. Characteristics and factors associated with intraocular lens tilt and decentration after cataract surgery. J Cataract Refract Surg. 2020;46(8):1126–31.
52. Mutlu FM, Erdurman C, Sobaci G, Bayraktar MZ. Comparison of tilt and decentration of 1-piece and 3-piece hydrophobic acrylic intraocular lenses. J Cataract Refract Surg. 2005;31(2):343–7.
53. Crnej A, Hirnschall N, Nishi Y, et al. Impact of intraocular lens haptic design and orientation on decentration and tilt. J Cataract Refract Surg. 2011;37(10):1768–74.
54. Harrer A, Hirnschall N, Tabernero J, et al. Variability in angle kappa and its influence on higher-order aberrations in pseudophakic eyes. J Cataract Refract Surg. 2017;43(8):1015–9.
55. Findl O, Hirnschall N, Draschl P, Wiesinger J. Effect of manual capsulorhexis size and position on intraocular lens tilt, centration, and axial position. J Cataract Refract Surg. 2017;43(7):902–8.
56. Zhang F, Zhang J, Li W, et al. Correlative comparison of three ocular axes to tilt and Decentration of intraocular lens and their effects on visual acuity. Ophthalmic Res. 2020;63(2):165–73.
57. Hirnschall N, Findl O, Bayer N, et al. Sources of error in Toric intraocular lens power calculation. J Refract Surg. 2020;36(10):646–52.
58. Hirnschall N, Buehren T, Trost M, Findl O. Pilot evaluation of refractive prediction errors associated with a new method for ray-tracing-based intraocular lens power calculation. J Cataract Refract Surg. 2019;45(6):738–44.
59. Cornaggia A, Clerici LM, Felizietti M, Rossi T, Pandolfi A. A numerical model of capsulorhexis to assess the relevance of size and position of the rhexis on the IOL decentering and tilt. J Mech Behav Biomed Mater. 2021;114:104170.
60. Ding X, Wang Q, Xiang L, Chang P, Huang S, Zhao YE. Three-dimensional assessments of intraocular lens stability with high-speed swept-source optical coherence tomography. J Refract Surg. 2020;36(6):388–94.
61. Akkin C, Ozler SA, Mentes J. Tilt and decentration of bag-fixated intraocular lenses: a comparative study between capsulorhexis and envelope techniques. Doc Ophthalmol. 1994;87(3):199–209.
62. Kranitz K, Mihaltz K, Sandor GL, Takacs A, Knorz MC, Nagy ZZ. Intraocular lens tilt and decentration measured by Scheimpflug camera following manual or femtosecond laser-created continuous circular capsulotomy. J Refract Surg. 2012;28(4):259–63.
63. Auffarth GU, Friedmann E, Breyer D, et al. Stability and visual outcomes of the capsulotomy-fixated FEMTIS-IOL after automated femtosecond laser-assisted anterior capsulotomy. Am J Ophthalmol. 2021;225:27.
64. Holland D, Rufer F. [New intraocular lens designs for femtosecond laser-assisted cataract operations: chances and benefits]. Ophthalmologe. 2020;117(5):424–30.
65. Gangwani V, Hirnschall N, Koshy J, et al. Posterior capsule opacification and capsular bag performance of a microincision intraocular lens. J Cataract Refract Surg. 2011;37(11):1988–92.
66. Chen YA, Hirnschall N, Maedel S, Findl O. Misalignment of a novel single-piece acrylic intraocular lens in the first three months after surgery. Ophthalmic Res. 2014;51(2):104–8.
67. Petrovic MJ, Vulovic TS, Vulovic D, Janicijevic K, Petrovic M, Vujic D. Cataract surgery in patients with ocular pseudoexpholiation. Ann Ital Chir. 2013;84(6):611–5.
68. Maedel S, Hirnschall N, Chen YA, Findl O. Effect of heparin coating of a foldable intraocular lens

on inflammation and capsular bag performance after cataract surgery. J Cataract Refract Surg. 2013;39(12):1810–7.
69. Mayer CF, Hirnschall N, Wackernagel W, et al. Late dislocation of a hydrophilic intraocular lens: risk ratios for predisposing factors and incidence rates. Acta Ophthalmol. 2018;96(7):e897–e8.
70. Mayer-Xanthaki CF, Pregartner G, Hirnschall N, et al. Impact of intraocular lens characteristics on intraocular lens dislocation after cataract surgery. Br J Ophthalmol. 2020;105:1510.
71. Hayashi H, Hayashi K, Nakao F, Hayashi F. Anterior capsule contraction and intraocular lens dislocation in eyes with pseudoexfoliation syndrome. Br J Ophthalmol. 1998;82(12):1429–32.
72. Miyoshi T, Fujie S, Yoshida H, Iwamoto H, Tsukamoto H, Oshika T. Effects of capsular tension ring on surgical outcomes of premium intraocular lens in patients with suspected zonular weakness. PLoS One. 2020;15(2):e0228999.
73. Remon L, Siedlecki D, Cabeza-Gil I, Calvo B. Influence of material and haptic design on the mechanical stability of intraocular lenses by means of finite-element modeling. J Biomed Opt. 2018;23(3):1–10.
74. Hayashi K, Harada M, Hayashi H, Nakao F, Hayashi F. Decentration and tilt of polymethyl methacrylate, silicone, and acrylic soft intraocular lenses. Ophthalmology. 1997;104(5):793–8.
75. Auffarth GU, McCabe C, Wilcox M, Sims JC, Wesendahl TA, Apple DJ. Centration and fixation of silicone intraocular lenses: clinicopathological findings in human autopsy eyes. J Cataract Refract Surg. 1996;22(Suppl 2):1281–5.
76. Walkow T, Anders N, Pham DT, Wollensak J. Causes of severe decentration and subluxation of intraocular lenses. Graefes Arch Clin Exp Ophthalmol. 1998;236(1):9–12.
77. Sato T, Shibata S, Yoshida M, Hayashi K. Short-term dynamics after single- and three-piece acrylic intraocular lens implantation: a swept-source anterior segment optical coherence tomography study. Sci Rep. 2018;8(1):10230.
78. Uzel MM, Ozates S, Koc M, Taslipinar Uzel AG, Yilmazbas P. Decentration and tilt of intraocular lens after posterior capsulotomy. Semin Ophthalmol. 2018;33(6):766–71.
79. Cinar E, Yuce B, Aslan F, Erbakan G, Kucukerdonmez C. Intraocular lens tilt and decentration after Nd:YAG laser posterior capsulotomy: femtosecond laser capsulorhexis versus manual capsulorhexis. J Cataract Refract Surg. 2019;45(11):1637–44.
80. Sauer T, Mester U. Tilt and decentration of an intraocular lens implanted in the ciliary sulcus after capsular bag defect during cataract surgery. Graefes Arch Clin Exp Ophthalmol. 2013;251(1):89–93.
81. Kemer Atik B, Altan C, Agca A, et al. The effect of intraocular lens tilt on visual outcomes in scleral-fixated intraocular lens implantation. Int Ophthalmol. 2020;40(3):717–24.
82. Yamane S, Sato S, Maruyama-Inoue M, Kadonosono K. Flanged Intrascleral intraocular lens fixation with double-needle technique. Ophthalmology. 2017;124(8):1136–42.
83. Kumar DA, Agarwal A, Agarwal A, Chandrasekar R, Priyanka V. Long-term assessment of tilt of glued intraocular lenses: an optical coherence tomography analysis 5 years after surgery. Ophthalmology. 2015;122(1):48–55.
84. Matsumura T, Takamura Y, Makita J, Kobori A, Inatani M. Influence of sclerotomy size on intraocular lens tilt after intrascleral intraocular lens fixation. J Cataract Refract Surg. 2019;45(10):1446–51.
85. Kurimori HY, Inoue M, Hirakata A. Adjustments of haptics length for tilted intraocular lens after intrascleral fixation. Am J Ophthalmol Case Rep. 2018;10:180–4.
86. Shuaib AM, El Sayed Y, Kamal A, El Sanabary Z, Elhilali H. Transscleral sutureless intraocular lens versus retropupillary iris-claw lens fixation for paediatric aphakia without capsular support: a randomized study. Acta Ophthalmol. 2019;97(6):e850–e9.
87. Mutlu FM, Bayer A, Erduman C, Bayraktar MZ. Comparison of tilt and decentration between phacoemulsification and phacotrabeculectomy. Ophthalmologica. 2005;219(1):26–9.
88. Iwama Y, Maeda N, Ikeda T, Nakashima H, Emi K. Impact of vitrectomy and air tamponade on aspheric intraocular lens tilt and decentration and ocular higher-order aberrations: phacovitrectomy versus cataract surgery. Jpn J Ophthalmol. 2020;64(4):359–66.
89. Ozates S, Kiziltoprak H, Koc M, Uzel MM, Teke MY. Intraocular lens position in combined phacoemulsification and vitreoretinal surgery. Retina. 2018;38(11):2207–13.
90. Leisser C, Hirnschall N, Findl O. Effect of air tamponade on tilt of the intraocular lens after Phacovitrectomy. Ophthalmologica. 2019;242(2):118–22.
91. Marcos S. Chapter 40: Slack incorporated. In: Hoffer K, editor. IOL power. 1st ed; 2011. p. 224.
92. Atchison DA. Refractive errors induced by displacement of intraocular lenses within the pseudophakic eye. Optom Vis Sci. 1989;66(3):146–52.
93. Kingslake R. Who? Discovered Coddington's equations? Opt Photonics News. 1994;5(8):20–3.